LASER CLADDING OF ASTROLOY ON INCONEL 718

C. Sainte-Catherine and M. Jeandin

Ecole Nationale Supérieure des Mines de Paris
Centre des Matériaux P.M. Fourt
B.P. 87, 91003, Evry Cedex
France

Abstract

The capability of solid-state lasers for cladding was investigated focusing on the study of significant microstructural features of the laser clad and the substrate. Both continuous-wave (CO_2 laser) and pulsed (CO_2 and Nd-YAG lasers) irradiations were tested. The melting of pre-deposited powder as well as powder flowing from a pneumatic delivery system were studied in relation to the laser and feed material parameters. Chemical and geometrical aspects of the Astroloy-Inconel 718 interface and the thermally affected zone (TAZ) were characterized. Microhardness measurements were in particular applied to the TAZ and the influence of post-annealing on the TAZ determined. The distribution of induced distorsions beneath the melted zone, exhibited by slip bands in Inconel 718 was estimated as a function of depth using a recently developped metallographic method.

Superalloy 718—Metallurgy and Applications
Edited by E.A. Loria
The Minerals, Metals & Materials Society, 1989

Introduction

Inconel 718 is currently used for applications ranging from low to high temperatures (1) due to its microstructure (2). It is mainly strengthened by γ" (DO_{22}) and γ' ($L1_2$) precipitates, creep ductility being governed by the intergranular precipitation of δ (DO_a).

The wide potential field of applications for alloy 718 often calls for improvements of the surface properties to meet with those required (3). Among all processes, cladding can be envisaged in particular for applications not only involving wear, erosion, corrosion but also for maintenance or repair inadequately machined parts. Cladding was therefore studied using Astroloy as a protective layer with Inconel 718 as the substrate. Astroloy is one of the best candidate material for cladding on alloy 718 so far as it exhibits better high temperature properties (e.g. the corrosion resistance) and is available in powder form which is very suitable for coating processes.

It is now well recognized that lasers offer a potential method of applying cladding alloys on substrates with low mixing and low residual deformation (4). Gas (CO_2) lasers have been extensively tested in the continuous wave mode processing and seem to be promising for cladding applications although at present they are only used in the laboratory. Solid state lasers (Nd-YAG) might however be more suitable for use in industry because of several prominent advantages such as beam handling by optical fibres due to the wavelength (1.06 μm against 10.6 μm for CO_2 lasers) or the reduced size of the device which allows convenient on-line installation and automation. Up-to-date the limited average output power (up to 400 W for commercial Nd-YAG lasers) prevented the use of solid-State Lasers for thermal surface treatments. However the development of so-called high power solid-state lasers (HPSSL), in particular within the frame of EUREKA projects in which this study has been carried out, should open the range of applications for HPSSL to the surface modification of materials (5- 7). This features a need for studies of the capability of processing with solid state lasers since these generally operate in the pulsed wave mode. Consequently, this work also investigated cladding on Inconel 718 using pulsed lasers.

Laser processing of superalloys dates back to the mid-seventies with, in particular, the so-called "Laserglaze" process (8). Since these impressive pioneering works, few studies have been devoted to this class of alloys (9) and especially 718 except for those by Mazumder et al. (3). However in every case, a CO_2 laser was used.

Materials and Apparatus

Materials

Conventional argon-atomized 400 mesh (after screening) Astroloy powder (chemical composition in Table I) was used as the clad material.

Table I. Chemical Composition of the Alloys, Wt.%.

	Cr	Fe	Co	Nb	Mo	Al	Ti	C	Others	Ni
Astroloy	15.3	-	17.1	-	5.3	4.2	3.5	0.05	0.15	Bal.
Inconel 718	18.0	18.1	0.47	5.1	3.0	0.4	0.9	0.03	0.25	Bal.

The substrate material was cast and wrought Inconel 718 (composition in Table I). The alloy has been heat-treated as follows :

955°C/1h/AC + 720°C/8h/FC + 650°C/8h/AC

which corresponded to a microhardness of about 390 15 Hv (with a load of 0.5 kg) and an average grain size of approximatively 130 µm (ASTM 4-5).

Lasers

Cladding was carried out using both Nd-YAG and CO_2 lasers, the characteristics of which are given in Table II.

Table II. Laser Characteristics

Laser	Nd-YAG	CO_2
Average output power (W)	250	3000
Output energy per pulse (J)	30	-
Pulse width (ms)	1-10	-
Spatial beam profile	multimode	TEM_{01}
Focal length (mm)	150 (lens)	150 (spherical mirror)

Processing

The CO_2 laser operated typically between 1 and 3 kW. Specimens of about 10 mm thick were traversed relative to the laser beam at speeds of approximately 0.5 to 2 m/min. Astroloy powder was either deposited onto Inconel 718 prior to the laser processing without binding compounds or delivered to the area of interaction by a pneumatic powder delivery system.

The main laser cladding parameters are shown in Table III.

Microstructural Study

The specimens were characterized by optical, scanning electron microscopy (SEM) coupled with energy dispersive spectrometry (EDS) and microhardness measurements. Conventional polishing and etching procedures were applied to transverse and longitudinal sections of the beam paths, i.e. sectioning and grinding from 1200 grit and then mechanically polishing to 1 µm diamond finish. In addition, for certain specimens, the distribution of the thermally induced distorsions beneath the melted zone was determined using the method developed at the "Ecole des Mines" by Clavel et al. (10).

Preliminary microstructural observations of C1 specimen (continuous wave processed with CO_2 lasers) in order to establish some typical features governing the material under irradiation.

Table III. Laser Processing Parameters

Sample Reference	C1	N1	C2	C3	C4	C5
Laser used	CO_2	Nd-YAG	CO_2	CO_2	CO_2	CO_2
Processing mode*	CW	PW	PW	PW	PW	PW
Power density (10^8 W/m^2)	2.5	20	4	5	5	5
Energy density (10^6 J/m^2. pulse)	-	4	4	5	10	10
Interaction time (ms)	100	2	10	10	20	20
Pulse rate (Hz)	-	10	17	17	20	25
Powder delivery** system	no	no	yes	yes	yes	yes
Traverse speed (m/min)	2.0	0.3	1.0	1.0	1.0	1.0

* CW : continuous wave
PW : pulsed wave
** with a flow rate of 11 g/s for Astroloy powder.

C1 microstructure. The study concentrated on single beam pass specimens exhibiting a semi-cylindrical homogeneous clad Astroloy layer, see Fig. 1a.

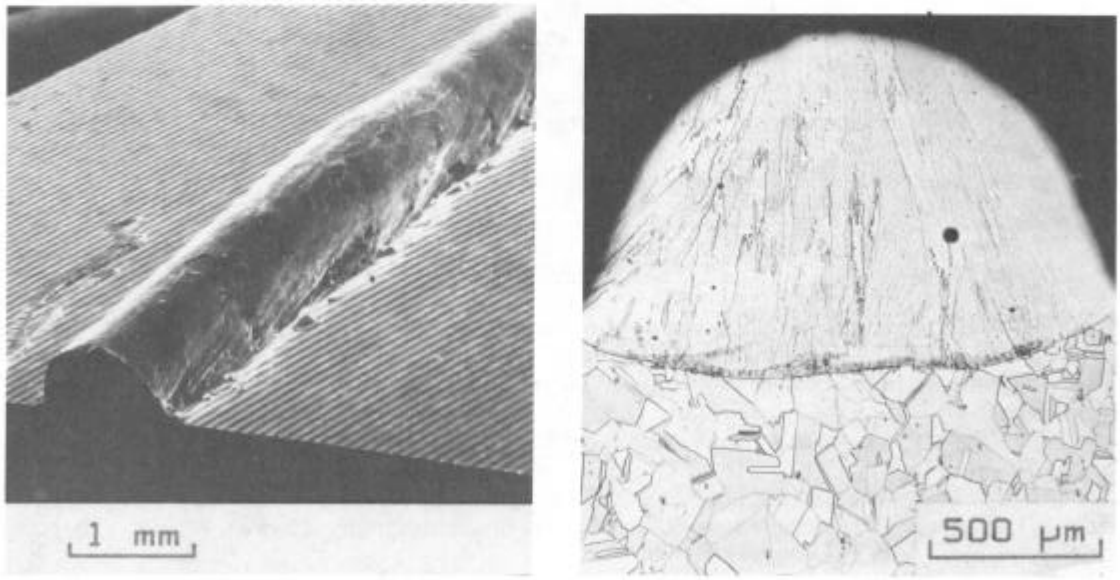

a b

Figure 1 - a) SEM image of a one beam pass clad region b) Optical image of C1 specimen transervse section.

Transverse sections of the cladding (Fig. 1b) showed some isolated pores (with a maximum diameter of about 50 μm) and a rather small amount of remelted Inconel 718. It was a deliberate decision not to eliminate the porosity using a shielding gas for example as suggested in previous works (11). However, gas shielding which in this case was not used to simplify the process and make the interpretation of phenomena clearer, should be applied to industrial work to prevent surface contamination.

Decreasing the amount of remelted substrate, by reducing the laser power or the interaction time for example, led to a more independent and more cylindrical clad (Fig. 6b). It is due to changes in the wetting phenomena between Inconel 718 and molten Astroloy. This can be characterized when considered the so-called external shape Re and the interface ratio Ri :

$$Re = L/H \quad (1)$$

where L is the width of the clad and H is the external height, and :

$$Ri = L/P \quad (2)$$

with P for depth of the remelted Inconel 718.
The value of which was for C1 : Re = 1.9 and Ri = 11.6

C1 clad specimen exhibited a drop of microhardness just below the melted region (see Fig. 2a) due to dissolution of strengthening precipitates (γ' and γ'') which were probably heated above their solvus temperature (12). This assumption was confirmed by the fact that heat treating in the precipitation zone of γ'' (Fig. 3) regenerated the structure as ascertained by the corresponding hardness profile which was almost continuously flat (Fig. 2b).

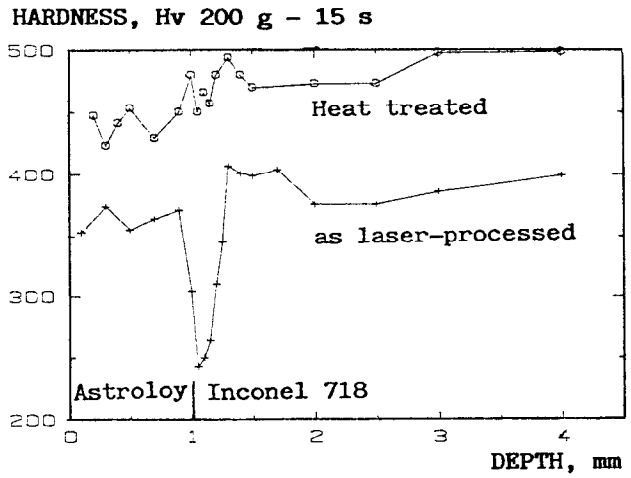

Figure 2 - Microhardness profiles of C1 specimen a) as laser-processed b) heat treated : 650°C/8h/AC.

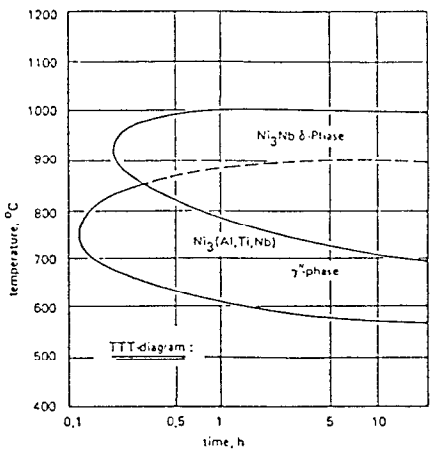

Figure 3 - Temperature-Time-Precipitation (TTP) diagram of Inconel 718, after (13).

The thickness of the mixing zone at the Astroloy-Inconel 718 interface was determined by EDS X-ray profile analyses (Fig. 4),using the Fe Kα1 (at 6.4 keV) and the Co Kα1 (at 6.93 keV) rays respectively typical of Inconel 718 and Astroloy. Depending on the location of the analysis, the thickness of the interfacial zone ranged between 20 and 50 microns.

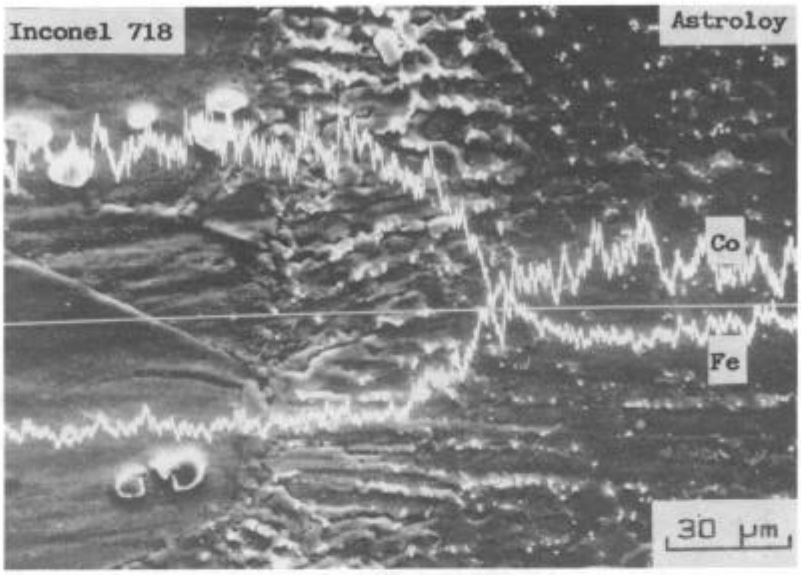

Figure 4 - SEM image of Inconel - Astroloy interface and corresponding X-ray profiles for C1 specimen.

Thermally induced distorsions. Plastic distorsions produce stacking sequences within γ" precipitates which can correspond locally with the stable δ phase sequence. Further aging (750°C/80h/AC) makes these deformation induced defects act as nuclei for δ growth which then appears as long platelets. Electrolytic etching of the heat-treated material reveals the δ platelets, the number of which is proportional to the plastic distorsion. This metallographic method must be however oonsidered as qualitative since a strict relation between the number of platelets and the level of plastic deformation is rather difficult to establish.

Dark field optical micrograph (Fig. 5) of the region below the molten material shows a platelet depleted zone of about 100 microns just beneath the interface. This reveals the absence of γ" precipitates as ascertained by the previously-described drop of microhardness. As expected, the platelets are less numerous when the distance from the interface is increased. The maximum thermally-induced distorsions are located towards the external interfaces and they can be compared to those due to conventional countersink by the observation of the non laser-processed regions which remained in the as-machined state.

Microstructures obtained by pulsed mode processing. N1 specimen (Fig. 6a) was achieved using powder pre-deposited without binding compounds onto the substrate surface prior to Nd-YAG laser processing.

When submitted to a pulse, powder is partly blown off and this left less powder for the subsequent pulse. A powder delivery system to achieve cladding with pulse mode processing was therefore used. However, the pulse rate was not high enough to lead to an homogeneous clad layer. The Astroloy coating formed by a succession of almost independent semi-spherical impacted drops. The particule temperature felt so quickly between two successive pulses which led to a discontinuous clad.

To achieve clad specimens to be compared with the C1 specimen more energy was needed per pulse than that when the Nd-YAG laser was used.

Consequently, in order to determine the parameters suitable for pulsed mode cladding, a CO_2 laser was operated in the pulsed mode which allowed higher energies and pulse rates.

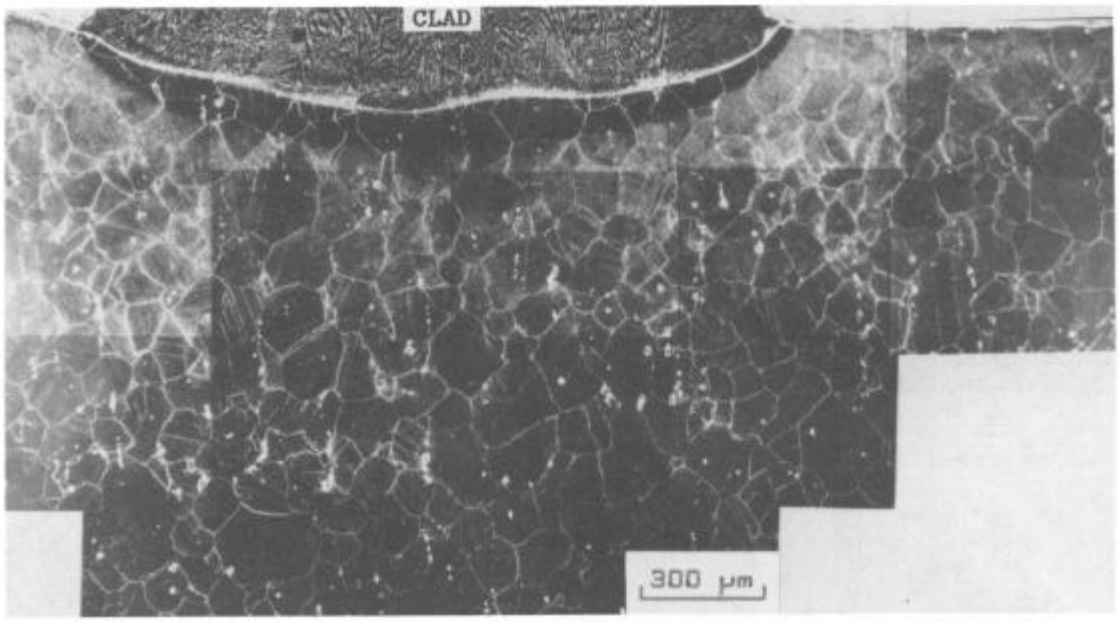

Figure 5 - δ platelets below the molten region for C1 specimen.

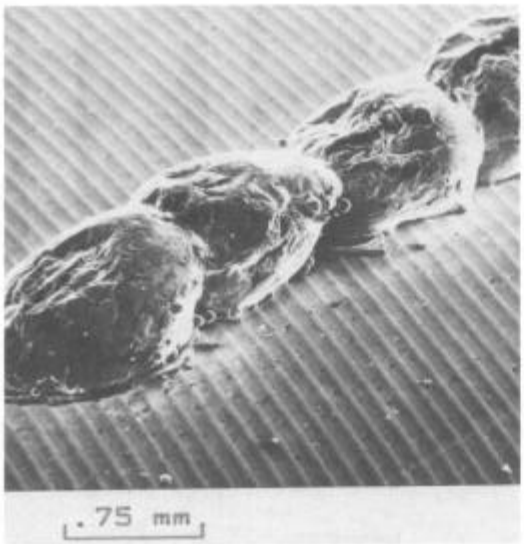

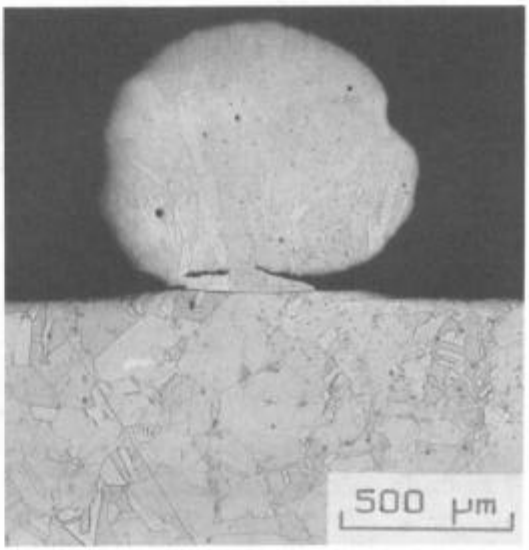

Figure 6 - Nd-YAG cladding, images of N1 specimens a) general view b) transverse section.

C2 to C5 specimens (Fig. 7) feature some crucial processing aspects. All the specimens were processed using different laser conditions, deliberatly chosen to isolate the effect of given parameters such as power, energy and pulse rate.

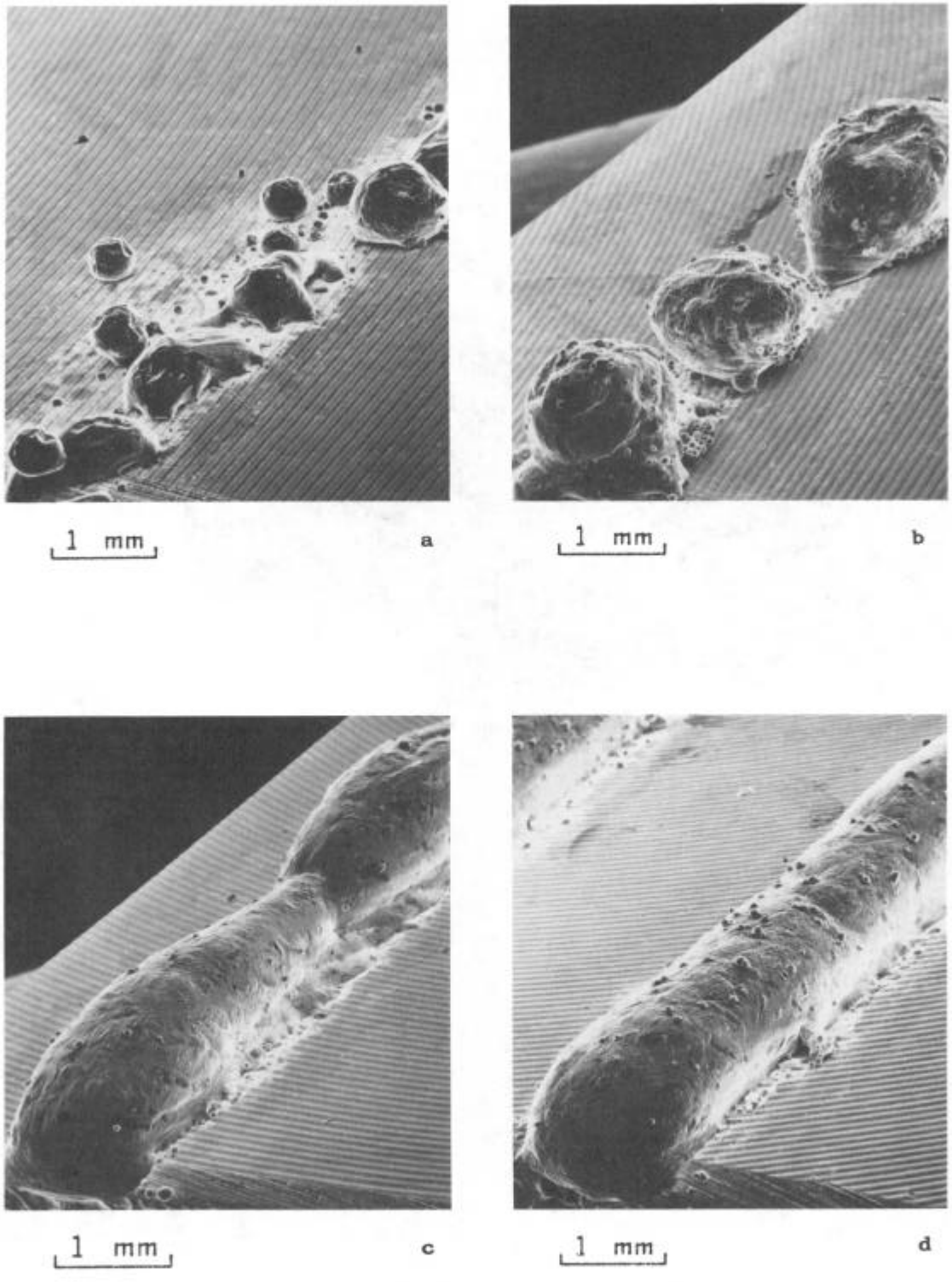

Figure 7 - SEM images of clad specimens processed using a pulsed CO_2 laser a) C2 specimen, starting conditions b) C3 specimen, influence of powder density c) and d) for respectively C4 and C5 specimens, influence of energy and pulse rate.

In certain conditions (those for C2 specimen), the drop often did not stick to the substrate and some powder in the laser path remained solid. When increasing power (C3 specimen, Fig. 7b) the majority of the irradiated powder stuck well to Inconel 718. To make the clad homogeneous, that is to prevent the formation of separate drops, the pulse rate had to be increased. The distance covered during the dead time t_d is $d = v.t_d$ with

$$t_d = 1/f - t_p \qquad (3)$$

where v is the transverse speed, f is the pulse rate and t_p the pulse duration (or the interaction time in table III). In the case of C3 specimen, the distance d was about 0.8 mm, thus lower than the laser beam diameter (3 mm). The separation of the drops was due to the large solidification shrinkage of the powder. Inconel 718 did not melt in the case of C3 specimen. The laser could not directly melt the substrate but it could provide a sufficient overheating of Astroloy to melt the proper part of the substrate.

Increasing the energy per pulse by enlarging the pulse width to ensure overheating of the Astroloy and raising the pulse rate to compensate for a over large shrinkage, improved the quality of the clad (C4 specimen, Fig. 7c). However, the dead time was not sufficiantly regulated to balance the shrinkage effect. Reducing the dead time led to structures comparable to those obtained by continuous wave processing (C5 specimen, Fig. 7d). Moreover, porosity is comparable to that of CW materials. The previously-defined geometrical coefficents were for C5 specimen : Re = 1.7 and Ri = 16.7. The internal ratio was higher than of C1 specimen and was probably at the origin of the two cracks observed under the clad in figure 8.

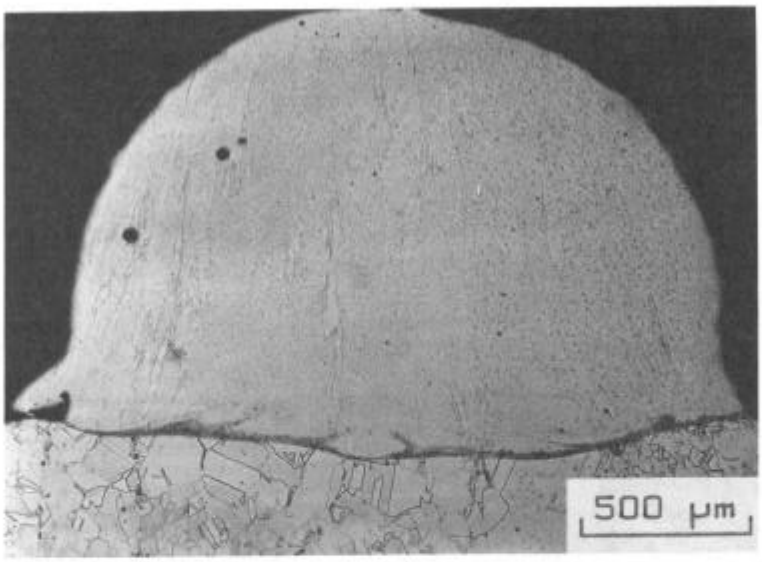

Figure 8 - Transverse section of C5 specimen.

It would be appropriate to comment here that the laser parameters have not a direct influence on the result but on material behaviour such as surface tension, oveheating of Astroloy or powder shrinkage.

Conclusion

Laser cladding is possible in a pulsed processing mode with parameters which be available with future high power solid state lasers. It is important to remember that solid state lasers have prominent advantages on CO_2 lasers such as beam handling by optical fibres for use in industry.

This preliminary study has only shown slight differences between the two processing modes (CW and PW) in terms of internal ratio and cracks at the interface. These are perhaps related and function of the clad volumes. More accurate comparisons (between heat affected zones, induced distorsions, mixed zones at the interface...) will be attempted with specimens with identical clad volumes and aspect ratios.

Acknowledegment - This work was made possible by the EUREKA-HPSSL Project and the constant support of SNECMA and CEA (Commissariat à l'Energie Atomique). The authors wish to thank ADALS (Association pour le Développement et les Applications du Laser à Solide) for their continued encouragement.

References

(1) Overview : "Superalloy 718 - a Look at the First 30 Years", J. Metals, 07, (1988), 35.

(2) J.W. Brooks and P.J. Bridges, "Metallurgical Stability of Inconel Alloy 718" in Superalloys 1988, Pub. by The Metallurgical Society, (1988), 33.

(3) J. Singh, K. Nagarthnam and J. Mazumder, "Oxydation Performance of Laser Clad NiCrAlHf Alloy on Inconel 718" in High Temperature Coatings, Orlando, Florida, USA, 7-9 Oct. 1986, Pub. AIME, USA, (1987), 101.

(4) C.G. Bruck, J. Metals, 02, (1987), 10.

(5) Eureka EU6-HPSSL, Final Report, Phase 0, (1987).

(6) C.L.M. Ireland, Laser Focus/Electro-Optics, 11, (1988), 49.

(7) A. Hoult et al., Industrial Laser Rev., 09, (1988), 7.

(8) E.M. Breinan et al., Superalloys - Metallurgy and Manufacture, Claitor's Publishing Division, Bâton Rouge, La., U.S.A., (1976).

(9) T. Puig et al., in Laser treatment of Materials, Edited by B.L. Mordike, Pub. DGM, FRG, (1987), 243.

(10) M. Clavel, D. Fournier and A. Pineau, Met. Trans., 6A, (1975), 2305.

(11) J. Singh and J. Mazumder, Mater. Sci. Technol., 2, (1986), 709.

(12) C. Sainte-Catherine, "Traitement de Surface du Nimonic 80A par Laser", Technical Report ETCA, Arcueil, France, (1986), (French).

(13) F. Shubert, in Phase Stability of High Temperature Alloys, V. Guttmann Ed., Applied Science Publishers Ltd, Ripple Road, England, (1981).